Multi-Watt mid-IR femtosecond polycrystalline Cr^{2+}:ZnS and Cr^{2+}:ZnSe laser amplifiers with the spectrum spanning 2.0–2.6 µm

Sergey Vasilyev,[1,*] Igor Moskalev,[1] Mike Mirov,[1] Sergey Mirov,[1,3] and Valentin Gapontsev[2]

[1]*IPG Photonics - Mid-Infrared Lasers, 1500 1st Ave N, Birmingham, AL 35203, USA*
[2]*IPG Photonics Corporation, 50 Old Webster Rd, Oxford, MA 01540, USA*
[3]*Center for Optical Sensors and Spectroscopies, University of Alabama at Birmingham, 1530 3rd Avenue South, Birmingham AL 35294, USA*
[*]*svasilyev@ipgphotonics.com*

Abstract: We demonstrate efficient amplification of few-optical-cycle mid-IR pulses in single-pass continuously pumped laser amplifiers based on polycrystalline Cr^{2+}:ZnS and Cr^{2+}:ZnSe. The 1.7 W output of a Kerr-lens mode-locked master oscillator at 2.4 µm central wavelength, 79 MHz repetition rate was amplified to 7.1 W and 2.7 W in Cr^{2+}:ZnS and Cr^{2+}:ZnSe, respectively. High peak power of the input pulses (0.5 MW) and high nonlinearity of the amplifiers' gain media resulted in a significant shortening of the output pulses and in spectral broadening. Transform-limited 40 fs pulses of the master oscillator were compressed to about 27–30 fs. The spectrum of the pulses was broadened from 136 nm to 450 nm (at −3 dB level); the span of the spectra exceeds 600 nm at −10 dB level.

References and links

1. L. D. DeLoach, R. H. Page, G. D. Wilke, S. A. Payne, and W. F. Krupke, "Transition metal-doped zinc chalcogenides: spectroscopy and laser demonstration of a new class of gain media," IEEE J. Quantum Electron. **32**(6), 885–895 (1996).
2. S. Mirov, V. Fedorov, D. Martyshkin, I. Moskalev, M. Mirov, and S. Vasilyev, "Progress in mid-IR lasers based on Cr and Fe doped II-VI chalcogenides," IEEE J. Sel. Top. Quantum Electron. **21**(1), 1601719 (2015).
3. S. Mirov, V. Fedorov, D. Martyshkin, I. Moskalev, M. Mirov and S. Vasilyev, "High average power Fe:ZnSe and Cr:ZnSe mid-IR solid state lasers," in Advanced Solid-State Lasers, OSA Technical Digest (online) (Optical Society of America, 2015), paper AW4A.1.
4. E. Sorokin, I. T. Sorokina, M. S. Mirov, V. V. Fedorov, I. S. Moskalev, and S. B. Mirov, "Ultrabroad continuous-wave tuning of ceramic Cr:ZnSe and Cr:ZnS lasers," in Lasers, Sources and Related Photonic Devices, OSA Technical Digest Series (CD) (Optical Society of America, 2010), paper AMC2.
5. I. T. Sorokina and E. Sorokin, "Femtosecond Cr^{2+}-based lasers," IEEE J. Sel. Top. Quantum Electron. **21**(1), 1601519 (2015).
6. T. Sorokina, E. Sorokin, and T. Carrig, "Femtosecond pulse generation from a SESAM mode-locked Cr:ZnSe laser," in Conference on Lasers and Electro-Optics/Quantum Electronics and Laser Science Conference and Photonic Applications Systems Technologies, Technical Digest (CD) (Optical Society of America, 2006), paper CMQ2.
7. E. Sorokin, N. Tolstik, K. I. Schaffers, and I. T. Sorokina, "Femtosecond SESAM-modelocked Cr:ZnS laser," Opt. Express **20**(27), 28947–28952 (2012).
8. M. N. Cizmeciyan, H. Cankaya, A. Kurt, and A. Sennaroglu, "Kerr-lens mode-locked femtosecond Cr^{2+}:ZnSe laser at 2420 nm," Opt. Lett. **34**(20), 3056–3058 (2009).
9. E. Sorokin, N. Tolstik, and I. T. Sorokina, "1 Watt femtosecond mid-IR Cr:ZnS laser," Proc. SPIE **8599**, 859916 (2013).
10. M. N. Cizmeciyan, J. W. Kim, S. Bae, B. H. Hong, F. Rotermund, and A. Sennaroglu, "Graphene mode-locked femtosecond Cr:ZnSe laser at 2500 nm," Opt. Lett. **38**(3), 341–343 (2013).
11. N. Tolstik, E. Sorokin, and I. T. Sorokina, "Graphene mode-locked Cr:ZnS laser with 41 fs pulse duration," Opt. Express **22**(5), 5564–5571 (2014).
12. S. Vasilyev, M. Mirov, and V. Gapontsev, "Kerr-lens mode-locked femtosecond polycrystalline Cr^{2+}:ZnS and Cr^{2+}:ZnSe lasers," Opt. Express **22**(5), 5118–5123 (2014).

13. S. Vasilyev, M. Mirov, and V. Gapontsev, "Mid-IR Kerr-lens mode-locked polycrystalline Cr^{2+}:ZnS laser with 0.5 MW peak power," in Advanced Solid State Lasers, OSA Technical Digest (online) (Optical Society of America, 2015), paper AW4A.3.
14. S. Vasilyev, I. Moskalev, M. Mirov, S. Mirov, and V. Gapontsev, "Three optical cycle mid-IR Kerr-lens mode-locked polycrystalline Cr^{2+}:ZnS laser," Opt. Lett. **40**(21), 5054–5057 (2015).
15. H. P. Wagner, M. Kühnelt, W. Langbein, and J. M. Hvam, "Dispersion of the second-order nonlinear susceptibility in ZnTe, ZnSe, and ZnS," Phys. Rev. B **58**(16), 10494–10501 (1998).
16. E. Yu. Morozov, A. A. Kaminskii, A. S. Chirkin, and D. B. Yusupov, "Second optical harmonic generation in nonlinear crystals with a disordered domain structure," JETP Lett. **73**(12), 647–650 (2001).
17. M. Baudrier-Raybaut, R. Haïdar, P. Kupecek, P. Lemasson, and E. Rosencher, "Random quasi-phase-matching in bulk polycrystalline isotropic nonlinear materials," Nature **432**(7015), 374–376 (2004).
18. M. Durand, A. Houard, K. Lim, A. Durécu, O. Vasseur, and M. Richardson, "Study of filamentation threshold in zinc selenide," Opt. Express **22**(5), 5852–5858 (2014).
19. H. Liang, P. Krogen, R. Grynko, O. Novak, C.-L. Chang, G. J. Stein, D. Weerawarne, B. Shim, F. X. Kärtner, and K.-H. Hong, "Three-octave-spanning supercontinuum generation and sub-two-cycle self-compression of mid-infrared filaments in dielectrics," Opt. Lett. **40**(6), 1069–1072 (2015).
20. S. Vasilyev, M. Mirov, and V. Gapontsev, "High power Kerr-lens mode-locked femtosecond mid-IR laser with efficient second harmonic generation in polycrystalline Cr^{2+}:ZnS and Cr^{2+}:ZnSe," in Advanced Solid State Lasers, OSA Technical Digest (online) (Optical Society of America, 2014), paper AM3A.3.
21. V. O. Smolski, S. Vasilyev, P. G. Schunemann, S. B. Mirov, and K. L. Vodopyanov, "Cr:ZnS laser-pumped subharmonic GaAs optical parametric oscillator with the spectrum spanning 3.6-5.6 µm," Opt. Lett. **40**(12), 2906–2908 (2015).
22. I. Pupeza, D. Sánchez, J. Zhang, N. Lilienfein, M. Seidel, N. Karpowicz, T. Paasch-Colberg, I. Znakovskaya, M. Pescher, W. Schweinberger, V. Pervak, E. Fill, O. Pronin, Z. Wei, F. Krausz, A. Apolonski, and J. Biegert, "High-power sub-two-cycle mid-infrared pulses at 100 MHz repetition rate," Nat. Photonics **9**, 721–724 (2015).

1. Introduction

Middle-infrared (mid-IR) lasers are in great demand for a variety of applications in life sciences and technology. Availability of femtosecond (fs) mid-IR laser sources with high average power and broad spectral span is an important prerequisite for high dynamic range molecular spectroscopy and hyperspectral imaging with the applications that range from fundamental science to environmental sensing, medicine, and industrial process control.

Transition-metal-doped II-VI semiconductors (TM:II-VI), introduced in the late 1990s [1], represent a viable route to high-power mid-IR lasing. TM:II-VI materials feature a favorable blend of parameters: a four-level energy structure, an absence of excited state absorption, close to 100% quantum efficiency of fluorescence (for Cr doped II-VI media), broad vibronic absorption and emission bands. Cr^{2+} and Fe^{2+} doped ZnS and ZnSe are the typical and most well-studied representatives of TM:II-VI family. Recent achievements in TM:II-VI laser technology include pulsed Fe^{2+}:ZnSe laser with 35 W average power at 4.1 µm wavelength and continuous wave (cw) Cr^{2+}:ZnSe laser with power in excess of 50 W at 2.4 µm wavelength [2, 3].

Cr^{2+} doped ZnS and ZnSe enable efficient room-temperature lasers with broad tuning over 1.9–3.3 µm range [2, 4]. Very conveniently, Cr^{2+}:ZnS/ZnSe can be pumped by efficient and reliable erbium (Er) and thulium (Tm) fiber lasers. Cr^{2+}:ZnS and Cr^{2+}:ZnSe have similar spectroscopic and laser parameters. Cr^{2+}:ZnS is regarded superior for high power laser applications due to better physical properties, while Cr^{2+}:ZnSe has higher nonlinearity. Both materials are available in single crystal and in polycrystalline forms. In most cases, polycrystalline laser gain elements allow to obtain superior laser parameters due to their better optical quality and higher dopant concentration [2].

Broad emission bands of TM:II-VI materials are favorable for generation of ultra-short mid-IR pulses. Ability to operate at room-temperature and availability of high power fiber lasers for optical pumping stimulated rapid progress of ultra-fast Cr^{2+}:ZnS/ZnSe lasers, as reviewed in [5]. Femtosecond Cr^{2+}:ZnS and Cr^{2+}:ZnSe lasers based on all major mode-locking techniques have been successfully implemented over the past decade including SESAM [6, 7], Kerr-lens [8, 9], and graphene [10, 11] mode-locked lasers. Recent demonstration of Kerr-lens mode-locked (KLM) lasers based on polycrystalline Cr^{2+}:ZnS and Cr^{2+}:ZnSe [12] has led to significant improvements in the output parameters of ultrafast mid-IR lasers in terms of average power (2 W) [2], pulse energy (24 nJ) [13], and pulse duration (≤29 fs) [14]. Thus, mode-locked Cr doped ZnSe and ZnS oscillators have come of age, and, arguably, represent

an appealing alternative to complex and inefficient ultra-fast mid-IR sources based on down-conversion of near-IR lasers, e.g. synchronously pumped optical parametric oscillators (OPO), optical parametric amplifiers (OPA) and difference frequency generation setups (DFG).

Zinc-blende semiconductors exhibit rather high second-order nonlinear susceptibility: 16 pm/V and 4 pm/V in ZnSe and ZnS, respectively, vs 15 pm/V in $LiNbO_3$ at 2.4 µm wavelength [15]. Polycrystalline Cr^{2+}:ZnS and Cr^{2+}:ZnSe gain media consist of a multitude of microscopic single-crystal grains. The broad distribution of grain sizes and orientations results in so-called random quasi-phase-matching (RQPM). The main distinctive features of RQPM are a linear dependence of the conversion yield with length of the medium and ultra-wide bandwidth [16, 17].

Another set of opportunities arises from high third order nonlinearly of ZnSe and ZnS. Nonlinear refractive indexes of these materials are approximately 50 times larger than that of CaF_2. The critical power for self-focusing is about 400 kW in bulk ZnSe and 430 kW in ZnS at 2.4 µm wavelength. Filamentation of mid-IR fs pulses in ZnSe and ZnS has attracted recent attention. The formation of filaments has been observed in ZnSe pumped well above the critical power by a kilohertz OPA tunable from 0.4 µm to 2.5 µm with 6–20 µJ pulse energy and ~30 fs pulse duration [18]. It was shown that the long-wavelength pumping is very favorable for the formation of filaments in ZnSe due to higher multiplicity of the multi-photon ionization (2.7 eV bandgap of ZnSe corresponds to six-photon ionization at 2.4 µm pump wavelength). The spectral broadening of about 450 nm was observed in ZnSe at 1.9–2.0 µm pump wavelength in five-photon ionization regime. More recently, 3-octave-spanning continuum has been obtained from filaments in ZnS (3.9 eV bandgap) pumped at 2.1 µm by a kilohertz 11 µJ, 27 fs OPCPA at about 1000 times the critical power for self-focusing [19].

Thus, the superb ultra-fast laser capabilities of Cr^{2+}:ZnS and Cr^{2+}ZnSe in combination with high second- and third-order nonlinearity of ZnS and ZnSe offer a number of unique possibilities. RQPM in polycrystalline Cr^{2+}:ZnS and Cr^{2+}ZnSe results in efficient second harmonic generation (SHG) directly in the gain element of KLM laser. Obtained SHG power (up to 250 mW) is high enough for some real-world applications [20]. The broad spectrum of SHG pulses (up to 22 THz [14],) suggests that they can be compressed to rather short durations. Other observed three-wave mixing effects include generation of third and fourth optical harmonics and sum frequency generation between mid-IR pulses and a cw pump beam. Obtained MW-level optical power inside the resonators of polycrystalline Cr^{2+}:ZnS/ZnSe KLM lasers opens an avenue for extension of ultra-fast laser oscillations beyond 3 µm range, e.g. via DFG or optical parametric oscillations in the gain element of KLM laser. On the other hand, high third-order nonlinearity of Cr^{2+}:ZnS and Cr^{2+}ZnSe may facilitate the implementation of KLM lasers with an octave-spanning spectra, e.g. strong spectral broadening arising from $\chi^{(3)}$ was reported for polycrystalline Cr^{2+}:ZnS KLM laser with 1.3 MW peak power inside the resonator, which is 3 times higher than the critical power for self-focusing [14].

2. Experimental setup and results

In this paper we report high average power, high repetition rate fs laser MOPAs based on polycrystalline Cr^{2+}:ZnS and Cr^{2+}ZnSe gain/nonlinear media. The experimental setup is illustrated in Fig. 1(a). As a master oscillator (MO) we used polycrystalline Cr^{2+}:ZnS KLM laser, which is described in detail in [13]. MO is optically pumped at 1567 nm by 8.4 W linearly polarized Er- doped fiber laser (EDFL) radiation. MO was operated at 79 MHz repetition rate with 22 nJ pulse energy, 1.7 W average power, and 40 fs pulse duration. The spectrum of MO pulses was $sech^2$ transform limited and centered at 2380 nm.

The amplifier stage is based on Cr^{2+}:ZnSe (Cr^{2+}ZnS) optically pumped at 1567 nm by another EDFL. AR coated polycrystalline Cr^{2+}:ZnS and Cr^{2+}:ZnSe gain elements were mounted at normal incidence between two curved mirrors and were cooled with room temperature water. Both gain elements were 9 mm long with ~5% low-signal transmission at the pump wavelength. The pump beam (Ø3.8 mm) was focused in the gain element by a lens

(L) with 80 mm focal length (focal spot Ø50 µm). MO and pump emissions were superimposed on a curved mirror HR[1] with high reflectivity in 2100–2700 nm range and high transmission at 1567 nm. The same mirror was used for focusing of MO emission in the gain element. The output beam was collimated by a curved mirror with protected gold coating and separated from the residual pump by another HR[1]. CaF$_2$ wedges on a flip mounts were used to split a part of the output for spectral and autocorrelation measurements.

Fig. 1. Experimental setup: (a) Schematic of polycrystalline Cr^{2+}:ZnS/Cr^{2+}:ZnSe fs laser MOPA; (b) optical setup for dispersion compensation of output pulses. MO – fs master oscillator (2380 nm central wavelength, 22 nJ pulse energy, 40 fs pulse duration, 79 MHz repetition rate); EDFL#1 – MO pump (Er- fiber laser at 1567 nm, 8.4 W), EDFL#2 – amplifier pump (Er- fiber laser at 1567 nm, 0–20 W); L –focusing lens, Cr:ZnS/ZnSe –polycrystalline gain element of the amplifier, HR[1] –dispersive high reflectors with GDD≈-200 fs^2, HR* – TOD compensator, W – CaF$_2$ wedge; DM – dichroic mirror for SHG separation with low GDD; YAG – stack of plane-parallel YAG plates; IAC – interferometric autocorrelator; Mono – grating monochromator.

Dispersion of the MOPA was controlled within 2200–2700 nm range. Input pulses were pre-chirped to compensate for dispersion in the master laser's output coupler (OC, 3.2 mm thick ZnSe substrate). The pre-chirping optics included: the high-reflector HR[1] with negative group delay dispersion GDD ≈-200 fs^2 and TOD compensator HR* (TOD ≈-3000 fs^2). To compensate for dispersion in the amplifier's gain element, we de-chirped output pulses prior to their delivery to an autocorrelator, as shown in Fig. 1(b). Output dispersion control included second dispersive high reflector HR[1]; dichroic mirror (DM) to separate SHG radiation, second TOD compensator HR*, and a combination of plane-parallel YAG plates.

Dispersion metrology in 2–3 µm range was not available. Therefore, dispersion of the gain elements, OC was calculated using the standard Sellmeier equations for undoped ZnS, ZnSe and YAG; the theoretical GDD spectra for the mirrors were provided by the coaters. Net GDD spectra of the MOPAs based on Cr^{2+}:ZnS and Cr^{2+}ZnSe are shown in Fig. 2.
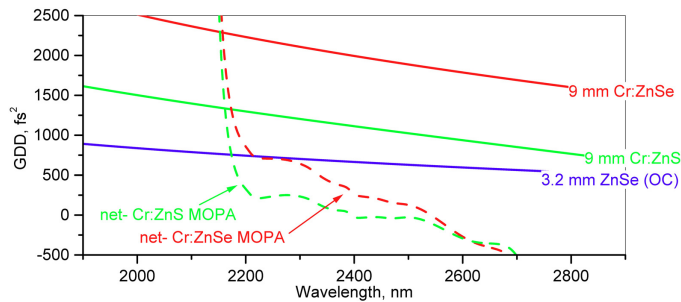

Fig. 2. Dispersion control in fs laser MOPA: solid lines show GDD spectra of 9 mm thick ZnSe and ZnS (gain elements), 3.2 mm thick ZnSe (substrate of the master laser's OC); dashed lines show net GDD of the MOPAs equipped with Cr^{2+}:ZnSe and Cr^{2+}:ZnS. The dispersion control components include 2 × HR[1], 2 × HR*, 12 mm YAG stack (for Cr^{2+}:ZnSe) or 8 mm YAG stack (for Cr^{2+}:ZnS). All spectra are theoretical, see main text and Fig. 1.

The spectra are calculated taking into account the pre-chirping components as well as the de-chirping components, which were installed before the autocorrelator. Figure 2 also shows dispersion curves for 9 mm thick Cr^{2+}:ZnS/ZnSe gain elements and for 3.2 mm thick ZnSe substrate of the OC.

Spectral parameters of the MOPA were characterized using a 0.15 m dual grating monochromator. The spectra were acquired using a lock-in amplifier and a PbSe detector (Thorlabs PDA20H). We did not post-process the spectra to account for wavelength dependences of the detector's responsivity and of the grating diffraction efficiency. Temporal parameters of the MOPA were evaluated using an interferometric autocorrelator (A·P·E GmbH). The experiments were carried out in standard lab environment at about 60% air humidity.

During the preliminary experiments we evaluated spectral broadening in bulk polycrystalline Cr^{2+}:ZnSe and Cr^{2+}:ZnS in passive regime, i.e. without optical pumping of the gain elements. Pulses from the master laser with 22 nJ energy and 40 fs duration (~480 kW peak power) were tightly focused (~Ø20 μm spot) in 9-mm long samples. The focusing was adjusted to obtain broadest spectra of output pulses. Results of the experiment are summarized in Fig. 3.
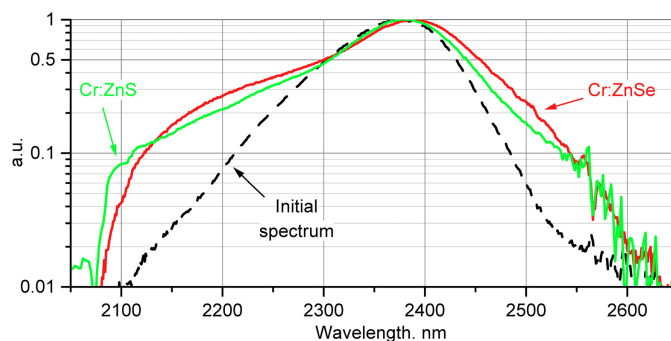

Fig. 3. Measured spectral broadening in bulk polycrystalline Cr^{2+}:ZnSe and Cr^{2+}:ZnS (9 mm thick samples, solid lines) and spectrum of input pulses (dashed line). $Sech^2$ transform-limited input pulses with ~480 kW peak power (22 nJ, 40 fs) were focused in ~Ø20 μm spot. The focusing was adjusted for broadest spectra of output pulses. All spectra are normalized to unity.

As can be seen, pumping of polycrystalline Cr^{2+}:ZnSe and Cr^{2+}:ZnS by fs mid-IR pulses at just above the critical power results in appearance of the wings in pulses spectra due to self-phase modulation. The broadening is about 10–20 nm (7–15%) at −3 dB and exceeds 150 nm (60%) at −10 dB. We explain the red-shift of the output spectra by absorption on Cr^{2+} centers.

In the consecutive experiments we engaged the optical pumping and characterized the output parameters of the Cr^{2+}:ZnSe and Cr^{2+}:ZnS amplifiers at different pump power levels. The size of the focal spot of the input beam from MO was increased to about Ø80 μm for better mode-matching with the pump beam.

Measured spectra of output pulses are shown in Fig. 4. At first we measured the spectra without pumping (dashed curves) and then we gradually increased the pump power (continuous curves). Maximum pump power was about 10 W for Cr^{2+}:ZnSe amplifier (was limited by optical damage of AR coatings of the gain element) and about 20 W for Cr^{2+}:ZnS amplifier. The spectra obtained at maximum pump power, are shown by thick solid lines. Numbers near the spectra correspond to measured average power at the amplifiers' output.

As can be seen, cw optical pumping of Cr^{2+}:ZnSe and Cr^{2+}:ZnS results in simultaneous amplification of fs pulses (like in conventional laser amplifier) and in their spectral broadening. Remarkably, the spectra of pulses became broader with an increase of cw pump power (e.g. an increase of the amplifier's gain). Thus, gain narrowing in the amplifier is overwhelmed by nonlinear interaction of pulses with the amplifier's gain medium. As a result, we obtained amplified pulses with 450 nm broad spectra (at full width half maximum, FWHM); the spectral span exceeds 600 nm at −10 dB.
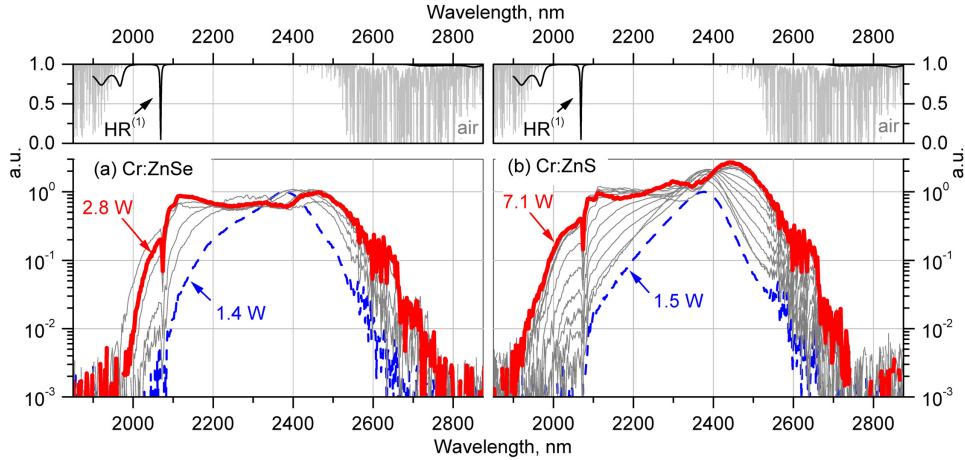
Fig. 4. Measured spectra of MOPAs equipped with (a) Cr^{2+}:ZnSe and (b) Cr^{2+}:ZnS gain elements. Dashed lines – initial spectra (pump is turned off); solid lines – the final spectra (highest reached power); grey lines – intermediate spectra (gradual increase of the amplifier's pump power). Initial spectra are normalized to unity. Final and intermediate spectra are normalized to optical power. Graphs in the top show transmission of 1.5 m standard air (grey background) and reflectivity of the pump separator HR[(1)].

Measured autocorrelations (ACs) of output pulses of Cr^{2+}:ZnSe and Cr^{2+}:ZnS MOPAs are shown in Fig. 5(a) and Fig. 5(b), respectively. Left and right graphs compare the ACs of 'cold' and 'hot' amplifiers, i.e. measured without pumping and at maximum pump power. Top and bottom graphs compare the ACs acquired with and without output dispersion compensation. The background noise in the ACs of 'hot' amplifiers is due to residual signal at pump wavelength. Duration of output pulses $\Delta\tau$ was estimated by $sech^2$ fit of the ACs using the autocorrelator's control software.
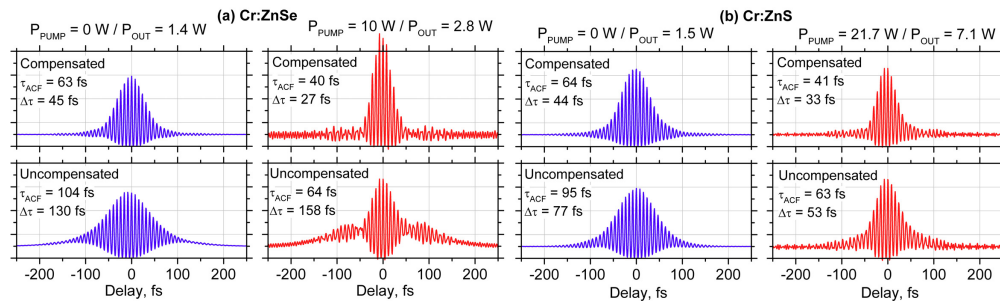

Fig. 5. Measured autocorrelations (ACs) of output pulses (a) Cr^{2+}:ZnSe MOPA and (b) Cr^{2+}:ZnS MOPA. ACs obtained with and without dispersion compensation (see Fig. 1b) are shown in the top and in the bottom, respectively. ACs obtained without pumping of the amplifier are shown on the left; ACs obtained at maximum pump power are shown on the right. P_{PUMP} is cw pump power; P_{OUT} is average output power of the MOPA; τ_{ACF} is a width of an AC and $\Delta\tau$ is a pulse duration obtained by $sech^2$ fit of an AC (both FWHM).

Comparison of the ACs of 'cold' amplifiers, which were obtained with and without output dispersion compensation, shows that the dispersion management of the MOPAs is fairly good but not perfect: 40 fs input pulses were re-compressed to 45 fs output pulses. Comparison of the ACs of 'cold' and 'hot' amplifiers allow us to conclude that the amplification of fs pulses in single-pass Cr^{2+}:ZnSe/ZnS amplifier is supplemented by significant decrease of pulse duration from 45 fs to about 30 fs. Most likely, the actual pulses are shorter: (i) some temporal broadening is introduced by the beam splitter of our autocorrelator (see Fig. 6 and discussion in [14]); (ii) dispersion control of the MOPA can be further improved; (iii) one can estimate

16 fs pulses taking into account 450 nm broad spectra at 2300 nm central wavelength and assuming, e.g., 0.4 time-bandwidth product.

Parameters of Cr^{2+}:ZnSe and Cr^{2+}:ZnS MOPAs as functions of pump power P_{PUMP} are illustrated in Fig. 6. Figures 6(a)–6(c) show respectively the amplifier's gain, spectral bandwidth at −10 dB level, and approximate pulse duration. The gain was defined as $G = P_{OUT}(P_{PUMP})/P_{OUT}(0)$ there P_{OUT} is output power of the MOPA. The gain was measured in mode-locked regime of the master oscillator (shown in Fig. 6(a) by symbols) and in cw regime (shown in Fig. 6(a) by dashed lines). As can be seen, the gains of fs and cw MOPAs almost coincide in a range of pump powers. Increase of the pump power within this range results in gradual broadening the spectra and decrease of pulse duration. At certain pump power the spectral width reaches maximum as shown in Fig. 6(b) by asterisks ($P^*_{PUMP} = 6.5$ W for Cr^{2+}:ZnSe, $P^*_{PUMP} = 17.5$ W for Cr^{2+}:ZnS). Pumping of the fs amplifier above this level results in: (i) roll-off of the gain (if compared to cw amplifier); (ii) some decrease and then constancy of the spectral width; (iii) constancy and then some increase of the pulse duration.
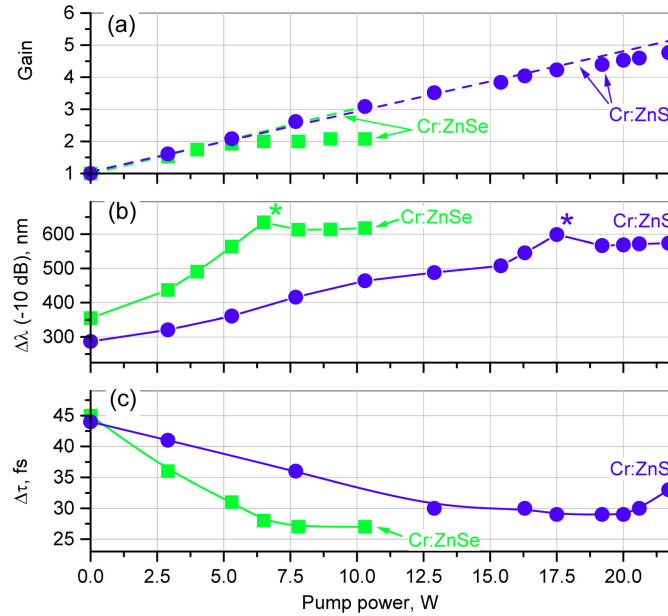

Fig. 6. Output characteristics of Cr^{2+}:ZnSe (■) and Cr^{2+}:ZnS (●) MOPAs vs pump power (P_{PUMP}): (a) gain of the amplifier, (b) spectral bandwidth $\Delta\lambda$ (at −10 dB level), (c) pulse duration $\Delta\tau$. The gain is defined as $G = P_{OUT}(P_{PUMP})/P_{OUT}(0)$ there P_{OUT} is average output power. $P_{OUT}(0) = 1.35$ W and 1.49 W for Cr^{2+}:ZnSe and Cr^{2+}:ZnS MOPAs, respectively. Dashed lines in part (a) correspond to the gain measured in cw regime of the MO.

Cr^{2+}:ZnSe and Cr^{2+}:ZnS gain elements were tested in similar conditions, which allows for some comparisons. Figure 6 shows that spectral broadening in Cr^{2+}:ZnSe is more pronounced, which can be attributed to higher nonlinearity of the material. On the other hand, the gain roll-off in Cr^{2+}:ZnSe occurs at relatively low pump power and limits the output power of the amplifier in fs regime. Probably, lower roll-off threshold in Cr^{2+}:ZnSe can be explained by relatively narrow bandgap (2.7 eV in ZnSe vs 3.6 eV in ZnS) and, hence, lower multiplicity of the multi-photon ionization. Further study is required to confirm the relationship between the multi-photon ionization in Cr^{2+}:ZnSe/ZnS and observed roll-off effects.

Output characteristics of Cr^{2+}:ZnSe and Cr^{2+}:ZnS mid-IR fs MOPAs are summarized in Table 1. Two sets of parameters in the table correspond to the broadest spectra and to the highest average power of output pulses. Pumping of Cr^{2+}:ZnSe amplifier was limited to 10.3 W due to the damage of AR coatings. Pump power of Cr^{2+}:ZnS amplifier was limited by available EDFL power.

Table 1. Output parameters of single-pass fs MOPAs[a]

Material	Broadest spectrum				Highest power			
	P_{PUMP}	P_{OUT}	$\Delta\lambda$	$\Delta\tau$	P_{PUMP}	P_{OUT}	$\Delta\lambda$	$\Delta\tau$
Cr^{2+}:ZnSe	6.5	2.6	635	28	10.3	2.8	618	27
Cr^{2+}:ZnS	17.5	6.3	599	29	21.7	7.1	574	33

[a]P_{PUMP} pump power (W), P_{OUT} average output power (W), $\Delta\lambda$ width of pulses spectrum at −10 dB level (nm), $\Delta\tau$ approximate pulse duration (fs) obtained by $sech^2$ fit of interferometric autocorrelation.

3. Conclusion

In summary, we implemented simple and robust single-pass fs mid-IR amplifiers based on polycrystalline Cr^{2+}:ZnSe and Cr^{2+}:ZnS. The amplifiers are pumped by low-cost cw EDFL, operate at full repetition rate of the master oscillator, and feature simultaneous amplification, spectral broadening, and compression of input pulses. We obtained output pulses with 7.1 W average power (at 79 MHz repetition rate), 574 nm broad spectrum (at −10 dB), and 33 fs pulse duration (conservative estimate) from the single-pass Cr^{2+}:ZnS amplifier. Conversion efficiency of cw pump radiation at 1.57 µm to few-optical-cycle mid-IR pulses at 2.4 µm was about 26% (31% of the absorbed pump power). Broader spectrum (> 600 nm) and shorter pulses (≤ 27 fs) with 2.8 W average power were obtained from the Cr^{2+}:ZnSe amplifier. To the best of our knowledge these are the shortest pulses with the highest average power reported to-date in the mid-IR.

There is little doubt that the output characteristics of the single-pass Cr^{2+}:ZnSe/Cr^{2+}:ZnS fs amplifiers can be further significantly improved by optimization of the input pulses (size of the beam, pre-chirping) and of the gain element (length, Cr^{2+} concentration). Very likely, better dispersion control of the amplifier will lead to rather short output pulses: 16 fs pulse duration (two optical cycles) can be estimated from the spectra assuming 0.4 time-bandwidth product. Synchronous pumping of single-pass Cr^{2+}:ZnSe/Cr^{2+}:ZnS amplifiers by available 1.5 µm picosecond and femtosecond fiber lasers may result in even shorter pulses with broader spectral span and higher pulse energy. Rigorous model of the amplifier, which takes into account an interplay between laser and nonlinear interactions of fs pulses with the gain medium, would be very helpful for mentioned above optimizations and improvements.

Availability of high power fs lasers at 2 – 3 µm is an important prerequisite for the development of mid-IR sources that span the spectrum over 3 – 10 µm. Approaches to high power coherent sources, which cover the whole mid-IR range include multi-octave continuum generation in bulk dielectrics and semiconductors [19], synchronously pumped OPO [21] and DFG [22] setups.

Acknowledgment